Contractile function of detrusor smooth muscle from children with posterior urethral valves – the role of fibrosis

Navroop Johal[1], Kevin Cao[1], Callum Arthurs[2], Michael Millar[3], Christopher Thrasivoulou[4], Aamir Ahmed[2], Rita I Jabr[5], Dan Wood[6], Peter Cuckow[1], Christopher H Fry[7].

[1]Department of Urology, Great Ormond St Hospital for Sick Children and Institute of Child Health, UCL, London, UK; [2]Centre for Stem Cell and Regenerative Medicine, King's College London, UK; [3]Queen's Medical Research Institute, University of Edinburgh, UK; [4]Department of Cell and Developmental Biology, UCL, UK; [5]School of Biochemistry and Medical Sciences, University of Surrey, Guildford, UK; [6]Department of Urology, University College London Hospitals, London, UK; [7]School of Physiology, Pharmacology and Neuroscience, University of Bristol, UK.

Short title: Detrusor contractile function and fibrosis

Key words: Bladder, posterior urethral valves, detrusor contraction, fibrosis, Wnt-signalling

Address for correspondence:
Professor Christopher Fry
School of Physiology, Pharmacology and Neuroscience,
University of Bristol, Bristol BS8 1TD, UK.
Email: chris.fry@bristol.ac.uk

Word count: 2993 words.

Author contributions
Devised the study: PC, DW, CHF
Experimental planning: CHF, AA, RIJ
Contributed data: NJ, KC, CA, MM, CT
Raised funding: NJ, RIJ, CHF
Drafted the manuscript: CHF, RIJ
Edited and approved the final manuscript: All authors

Abstract:

Introduction

Posterior urethral valves (PUV) is the most common cause of congenital bladder outflow obstruction with persistent lower urinary tract and renal morbidities. There is a spectrum of functional bladder disorders ranging from hypertonia to bladder underactivity, but the aetiology of these clinical conditions remains unclear.

Aims and objectives

We tested the hypothesis that replacement of detrusor muscle with non-muscle cells and excessive deposition of connective tissue is an important factor in bladder dysfunction with PUV. We used isolated detrusor samples from children with PUV and undergoing primary or secondary procedures in comparison to age-matched data from children with functionally normal bladders. *In vitro* contractile properties, as well as passive stiffness, were measured and matched to histological assessment of muscle and connective tissue. We examined if a major pathway for fibrosis was altered in PUV tissue samples.

Methods

Isometric contractions were measured *in vitro* in response to either stimulation of motor nerves to detrusor or exposure to cholinergic and purinergic receptor agonists. Passive mechanical stiffness was measured by rapid stretching of the tissue and recording changes to muscle tension. Histology measured the relative amounts of detrusor muscle and connective tissue. Multiplex quantitative immunofluorescence labelling using five epitope markers was designed to determine cellular pathways, in particular the Wnt-signalling pathway, responsible for any changes to excessive deposition of connective tissue.

Results and Discussion

PUV tissue showed equally reduced contractile function to efferent nerve stimulation or exposure to contractile agonists. Passive muscle stiffness was increased in PUV tissue samples. The smooth muscle:connective tissue ratio was also diminished and mirrored the reduction of contractile function and the increase of passive stiffness. Immunofluorescence labelling showed in PUV samples increased expression of the matrix metalloproteinase, MMP-7; as well as cyclin-D1 expression suggesting cellular remodelling. However, elements of a fibrosis pathway associated with Wnt-signalling were either reduced (β-catenin) or unchanged (c-Myc). The accumulation of

extracellular matrix, containing collagen, will contribute to the reduced contractile performance of the bladder wall. It will also increase tissue stiffness that *in vivo* would lead to reduced filling compliance.

Conclusions

Replacement of smooth muscle with fibrosis is a major contributory factor in contractile dysfunction in the hypertonic PUV bladder. This suggests that a potential strategy to restore normal contractile and filling properties is development of the effective use of antifibrotic agents.

Introduction:

Posterior urethral valves (PUV) is the most frequent cause of congenital bladder outflow obstruction (BOO) in boys, with a prevalence of about 1:4,000 [1]. Functional lower urinary tract problems underpin the serious morbidity in PUV. Whilst the urethral obstruction is easily treated at birth, persistent bladder dysfunction with incontinence in 70-90% and end-stage renal failure in childhood remain significant morbidities [2]. Urodynamic studies of patients with PUV shows a spectrum of phenotypes and a sequence of hypertonia, flaccidity and myogenic failure that governs urological and renal care [3]. Animal models of fetal sheep and rabbit partial bladder outflow obstruction have been developed to investigate the pathophysiology of bladder dysfunction in patients [4-6]. Most studies have succeeded in developing large compliance bladders [5,6], although in one urodynamic study measurements were interpreted as a low compliance bladder [4]. A study with fetal sheep used a shorter obstruction period of nine days, in contrast to 30 days normally used, to determine if a low compliance bladder represented an earlier, compensated phase before a decompensated, high compliance, flaccid state was generated [7]. Although there was bladder hypertrophy, there was no increase of bladder wall stiffness and in some instances there was progression to a high compliance vessel even with this short period of BOO.

The questions therefore remains if animal models can effectively reproduce the human neonatal phenotype of a low capacity, poorly compliant bladder and if human tissue studies may provide additional insight. We have shown previously that bladder wall tissue from children undergoing primary or secondary repair procedures for bladder exstrophy remains viable to carry out *in vitro* experiments [8]. Tissue from exstrophy bladders was stiffer but poorly contractile, explained by replacement of detrusor with fibrotic tissue, but remaining smooth muscle functioned normally.

Fibrosis is mediated by activation of transforming growth factor-β (TGF-β) receptors [9], in turn regulated by the Wnt-signalling network via β-catenin. β-catenin is a pivotal component of Wnt signalling, as a transcription factor it promotes transcription of three key target genes; *C-Myc* [10], which encodes the transcription factor cMyc; *CCND-1*, which encodes the cell cycle regulator cyclin-D1, and *MMP-7* gene, which encodes for matrix metalloproteinase MMP-7 protein, with overall effects of driving cellular proliferation and tissue re-modelling,. Kidney fibrosis has been extensively investigated, but mechanisms involved in bladder fibrosis less so. Renal fibrosis induced by unilateral ureteric obstruction is associated with increased c-Myc expression and fibroblast activation [11]. Hypertension-induced kidney fibrosis is associated with upregulation of β-catenin and cyclin-D1 expression [12]. MMPs also determine the extent of fibrosis and expression of MMPs is regulated by the Wnt-β-catenin pathway with the involvement of the TGF-β receptor [13]. We hypothesised that with PUV excessive fibrosis in the bladder wall contributes to reduced contractile function, a process regulated by Wnt-dependent pathways.

Methods

Tissue samples, ethics and preparations. Bladder biopsy samples were collected from patients with normal bladder function (*n*=18; 13M, 5F) or with PUV (*n*=14; 14M). The age and gender of each patient and the procedure undergone, as well as the experiments undertaken with each biopsy are listed (Table 1). Ethical approval was granted by the UK Human Research Authority and the study accepted by the Great Ormond Street Hospital R&D department. Informed consent was obtained from parents, guardians or Gillick-competent minors. Biopsy samples were from the anterior bladder wall, or the superior wall in the case of renal transplants, and without evidence of adjacent metaplasia in the one case of tumour excision. Samples were stored in Ca^{2+}-free Tyrode's solution and used within 15 minutes. Mucosa was discarded after blunt dissection and tissue divided into pieces for 1) histology and immunohistochemistry, stored overnight in 4% paraformaldehyde at 4°C and 2) *in vitro* functional experiments that were started within one hour.

Solutions. Functional experiments were carried out at 36±0.5°C in Tyrode's solution (mM): NaCl, 118; $NaHCO_3$, 24; KCl, 4.0; $MgCl_2$, 1.0; NaH_2PO_4, 0.4; $CaCl_2$, 1.8; glucose, 6.1; Na pyruvate, 5.0; pH 7.4, 5%CO_2,95% O_2. Ca^{2+}-free solution was (mM): NaCl, 132; KCl, 4.0; NaH_2PO_4, 0.4; glucose, 6.1; Na pyruvate, 5.0; HEPES, 10.0, pH 7.4 with 1M NaOH. The muscarinic receptor agonist carbachol and antagonist atropine, as well as the purinergic receptor ($P2X_1$) agonist α,β methylene ATP (ABMA) were diluted from aqueous 1 or 10 mM stock solutions. All chemicals were from Sigma UK.

Active tension recording. Detrusor strips (1-2 mm diam; 4-9 mm length) were dissected from the sample and tied in a horizontal superfusion trough between an isometric force transducer and a fixed hook. Nerve-mediated contractions were elicited by electrical field stimulation (3-s trains, width 0.1ms, frequency 1-40Hz); abolished by 1μM tetrodotoxin. Contractions by direct muscle

stimulation were elicited by carbachol (0.1-30μM) or ABMA (10 μM). Tension amplitude data were normalised to cross-section area.

Histology. Fixed portions of the biopsy were serially dehydrated in ethanol, cleared in xylene and mounted in paraffin. At least three sections (5 μm) of each biopsy sample were mounted on TESPA-coated glass slides and stained with Verhoeff-van Gieson (collagen, red; elastin, black; muscle yellow/orange). Whole-slide images were captured with a Zeiss Axioscan Z1 (Zeiss, Cambridge, UK), filtered for noise on ImageJ and amounts of muscle and connective tissue (collagen and elastin) were quantified using colour thresholding, to produce a smooth muscle : connective tissue (SM:CT) ratio. Data from each triplicate of sections were averaged for a value of a particular sample.

Biomechanical measurements. Stress-strain relationships were recorded from normal (n=6) and PUV (n=5) muscle strips. Muscle strips were prepared as for active tension recording, except that the fixed hook was replaced by a rod, within a solenoid coil, that rotated in response to a potential difference (p.d.) applied across the solenoid. Application of a square-wave p.d. (100-s on-off) rapidly stretched the preparation with a consequent increase of passive tension which showed a partial visco-elastic relaxation to an eventual new steady-state level, $T1$ (see Figure 2A). $T1$ was derived by fitting the visco-elastic portion to a single declining exponential function to estimate an asymptotic value. The elastic modulus, E, a measure of tissue stiffness, was calculated from the relationship: $E = \sigma/\varepsilon$, where σ is the steady-state force, $T1$, or stress, developed in the tissue (mN/mm^2 cross-section area, kPa) in response to a proportional length change, strain (ε). ε varied between 0.06-0.28 (6-28% of resting length), to avoid excessive length changes where the stress-strain relationship becomes non-linear.

Multiplex immunofluorescence labelling and quantitative image intensity analyses. A tissue array was constructed from formalin-fixed paraffin-embedded tissue blocks. Tissue cores (1mm diam) were moved to a recipient block and sectioned (4 μm). Antibodies for MMP-7 (ab4044, Abcam), cyclin-D1 (sc 718, Santa Cruz), β-catenin (ab22656, Abcam) and c-Myc (Novacastra/Leica Biosystems) were optimised for concentration, pH-dependence and antigen retrieval. A BondmaX™ automated system (Leica BioSystems) comprised an automated staining platform [14]; the identity of antibodies or configuration of tissue in the array was blinded to the researcher. Multiplex staining was conducted according to manufacturer's recommendations and the following fluorescent labels were used: Cy3 (514/565 nm, yellow, MMP-7), Cy5 (633/671 nm, purple, cyclin-D1), FITC (488/517 nm, green, β-catenin), Cy3.5 (561/617 nm, red, c-Myc) respectively, as well as the nuclear counter-stain DAPI (405/429 nm, blue). For expression analysis each section was imaged with a TCS SP8 confocal system (Leica) at x10, then x63, magnification. For co-localisation analysis x63 (x6 digital zoom, 0.17 μm z-step) images were taken from three, random areas of each section and analysed using Huygens professional image deconvolution software (Scientific Volume Imaging, Hilversum, NL) [14] using a macro compiled to measure individual intensities. Co-localisation of two labels in adjacent pixels was calculated as a Global Intersection Coefficient.

Data presentation and analysis. Data are mean±SEM, except for image analysis and elastic modulus data sets that are shown as median [25,75% interquartiles], *N*=number of biopsies; *n*=number of preparations or sections. Significances between multiple data sets used ANOVA, followed by appropriate parametric or non-parametric *post hoc* tests; the null hypothesis was rejected at *p<0.05, **p<0.01, ***p<0.001. Concentration-response or force-frequency curves were fitted to: $T=(T_{max}.x^n)/(x^n+k_m^n)$: where T_{max} is, maximum response at high stimulation

frequency (*f*) or agonist concentration (*S*); *x* is, different values of *f* or *S*; k_m is, value of *x* required to achieve $T_{max}/2$; *n* is, a

Results

Nerve-mediated and agonist-induced contractions; tissue histology. Detrusor preparations generated frequency-dependent contractions to electrical field stimulation (Figure 1A). Those from PUV patients were significantly smaller than those from normal bladders, including the $T_{max,EFS}$ value. The frequency for half-maximal contraction, $f_{1/2}$, was not significantly different between the two groups – see Table 2. Atropine-resistant contractions were recorded in both groups: the percentage of contraction remaining after 1 μM atropine was similar in both groups. All samples also responded to the contractile agonists carbachol (0.1-30 μM) and α,β methylene-ATP (10 μM). Concentration-response curves to carbachol were constructed and pEC_{50} (-logEC_{50}) values as well as maximum estimated contraction, $T_{max,c}$, were determined (Figure 1B). $T_{max,c}$ was also smaller in the PUV group, but pEC_{50} values were similar. Responses to a single concentration of ABMA (10 μM) were also significantly smaller in the PUV group (Table 2). A reduction of the $T_{max,EFS}$:$T_{max,c}$ ratio is used to estimate the magnitude of functional denervation in a preparation: in our analysis there was no such significant change to the ratio. Analysis of sections stained with Verhoeff-van Gieson reagent showed that smooth muscle and collagen comprised the great bulk of the tissue sections. Samples from PUV patients had a significantly smaller smooth muscle/connective tissue (SM/CT) ratio compared to tissue from normally functioning bladders (Table 2), sample sections stained with Verhoeff-van Gieson showed more collagen in the PUV section (Figure 1C).

The age of the patient when samples were obtained is a confounding factor as both the SM/CT ratio and contractile tension increase with age in tissue from the normally functioning human paediatric bladder [15]. The median ages of patients from whom samples were obtained were not statistically different in normally-functioning and PUV bladders, but this included a wide range in both groups (see Table 1). With tissue from normally-functioning bladders there were significant relationships with age for $T_{max,EFS}$ values (r=0.75, p=0.02, n=9) and SM/CT ratio (r=0.70, p=0.02, n=11). Other contractile variables in Table 2 showed no significant relationships with age. For data from the PUV group there were no significant relationships with age.

Biomechanical properties. Increased tissue collagen will impact on passive mechanical properties and was tested by measuring the elastic modulus in a separate series of experiments. Figure 2A shows a sample experiment of stress changes after a series of strains ranging from 8 to 20% of the resting length. At least three stress-strain cycles were imposed for each strain change and a feature was that the first in each set often generated more stress than the remainder (Figure 2B). In the subsequent analysis the first cycle was not used for analysis and the example of Figure 2A show the third cycle of each strain. Over the range of imposed strains, stress changes were approximately proportional to imposed strains. Figure 2C shows examples from PUV and normal bladder function tissue, fitted to a linear function, with the slope equivalent to tissue elastic modulus, E. Values of E from normally-functioning bladders were relatively similar in contrast to the wider range of values from PUV specimens where all but one were greater than control values. No significant relationships of elastic modulus with age were observed in the limited number of samples for the control and PUV groups.

Multiplex immunofluorescence labelling. High-power immunofluorescent images (x63; Figure 3A) were used for intensity analysis of protein expression for each of the five labels in the section and

also for co-localisation analysis. DAPI counts, as a nuclear stain, at low power were not different between normal and PUV samples ($9.68\pm1.55*10^8$ *vs* $9.93\pm1.47*10^8$ pixels per section; *N*=10,7), indicating that any alterations to other labels were not due to different numbers of cells. MMP-7 protein expression was significantly greater in PUV samples, as was cyclin-D1 expression. By contrast, there was a significant decrease of β-catenin and c-Myc expression in PUV samples (Figure 3B). Co-localisation analysis (Figure 3C) measured the proportion of intersecting pixels of two proteins, and although it does not necessarily represent functional interaction this analysis indicates the potential to do so. Greatest co-localisation with the nuclear marker DAPI was shown for MMP-7 and was maintained in PUV samples. The cell cycle regulator, cyclin D-1 showed greater co-localisation in PUV samples with the DAPI label, with MMP-7 and also with the transcription factors β-catenin and c-Myc.

Discussion

Contractile function of PUV bladder wall tissue. Force generated by electrical field stimulation of PUV bladder tissue was significantly less than from normal bladder preparations. Several reasons could explain this reduction: denervation of detrusor by excitatory efferent nerves; reduced response to neurotransmitters; dysfunctional excitation-coupling in detrusor myocytes; replacement of detrusor muscle with non-contractile cells or extracellular matrix. Functional denervation is unlikely as carbachol-mediated contraction was similarly reduced. i.e. the $T_{max,EFS}$:$T_{max,carb}$ ratio was unchanged (Table 2). It is also unlikely that acetylcholine potency, the principal excitatory neurotransmitter, is less as carbachol pEC_{50} was similar in normal and PUV bladder samples. There is a similar potency to muscarinic agonists in tissue from adult patients with normal and overactive bladders [16], but contrasts with a super-sensitivity in fetal rabbits

with BOO [17]. Replacement of detrusor muscle with other cellular material or increased extracellular matrix is a major reason for contractile failure in human exstrophy tissue [8]. Histological examination showed a similar decrease of the smooth muscle content in PUV samples. Assuming these are the two main tissue components, Table 2 data show a similar mean reduction of both smooth muscle mass (40%) and maximum response to carbachol (47%). There is also possible dysfunction of excitation-contraction coupling in remaining myocytes. This was not tested directly with PUV biopsy samples, due to their relatively small size. However, with human exstrophy bladder samples it was shown that intracellular [Ca^{2+}] responses to contractile agonists were maintained [8]. Of interest, ABMA responses declined more in PUV samples compared to carbachol responses. $P2X_1$ receptor density in adult obstructed bladders is unaltered or actually increases [18,19] but equivalent assays have not yet been done in paediatric tissue samples.

Biomechanical measurements. Increased connective tissue in PUV samples from this study was associated with a greater tissue stiffness, quantified by the elastic modulus, *E*. The range of values in the PUV group was very variable, most much greater than the normal bladder cohort. Moreover, one value was smaller from a patient who had a kidney transplant several years previously. Urodynamic studies show that filling compliance evolves in PUV patients from low to high values as the PUV bladder decompensates [20]. However, the greater median stiffness in these samples is consistent with the interpretation that most samples were not taken from decompensated bladders, a situation difficult to achieve with animal models [21]. However, it demonstrates that the paediatric PUV bladder does not always rapidly become a decompensated, high compliance organ. It remains an important goal to characterise, with a more comprehensive study, if the bladder generally evolves from a stiff phenotype to an over-compliant, decompensated organ, and what is the underlying tissue pathology.

Extracellular matrix has an important role to determine overall bladder wall stiffness; lamina propria thickness is crucial, as it contains a high collagen concentration. With fetal BOO there is a high cell turnover, resulting in remodelling of the detrusor layer and thickening of the lamina propria through addition of collagen and amorphous ground substance [22]. The shift from a low- to a high-compliance bladder with BOO may be due to the type of collagen and its quantity in a given volume of tissue. Type-! collagen is most abundant, but increased collagen type-III deposition accompanies BOO [23], one that reduces overall stiffness of mixed collagen fibrils, although both are stiffer than muscle [24]. With maintained BOO, collagen concentration decreases with greater amounts of amorphous ground substance resulting in a high-compliance bladder [25].

Age, fibrosis and contraction. The age-range of patients varied from as little as 1-2 months to over 150 months in both groups, although median ages were not significantly different. In a previous study, with tissue from normally-functioning human bladders, we showed an age-dependent increase of smooth muscle content and also *in vitro* nerve-mediated contractions [15]. In this study we confirmed these relationships, although agonist (carbachol- and ABMA)-dependent contractions did not show age-dependence. This difference may reflect different time-scales over which parasympathetic innervation and maturation of detrusor myocyte receptor density occur. In the PUV group no age-dependent associations with contraction magnitude or SM/CT ratio were observed. However, as two distinct cohorts it can be concluded that contractile function and smooth muscle proportion is reduced in the PUV group over a range of ages, compared to patients with normally-functioning bladders. The accumulation of further data will allow a test of the hypothesis that in the PUV group the normal age-dependent increase of smooth muscle content and contraction force does not occur.

Cell pathways mediating fibrosis. Wnt-signalling is pivotal during normal embryonic developmental stages and less active afterwards in many tissues. However, it maintains a role in stem cell maintenance and differentiation, as well as adult tissue remodelling and regeneration after injury. β-catenin is an important transducer of Wnt-signalling to facilitate gene transcription and regulates functions such as cell proliferation and differentiation. However, the reduced c-Myc and β-catenin expression in PUV, indicates that downregulation of the Wnt-signalling pathways in fibrosis may be associated with this anomaly, in contrast to that previously described for liver fibrosis [26]. The low co-localisation of β-catenin with nuclear markers or c-Myc is consistent with its cellular distribution in membrane, cytosolic and nuclear pools [27]. The total expression and distribution of the cell cycle regulator cyclin-D1 was also of interest; total expression was increased significantly in PUV, similar to that observed with renal and pulmonary fibrosis [12,27]. As β-catenin expression appears to be decreased, this would suggest cyclin-D1 transcription is activated via a signal other than the Wnt pathway [28]. Moreover, its substantially greater co-localisation with the nuclear marker, DAPI, and c-Myc suggests increased transcriptional activation. MMP-7 functions as an extracellular protease which degrades, among other targets, collagen-III (but not collagen-I), a subtype associated with fibrotic development in bladder outflow obstruction (BOO) models [29]. The observation of a high co-localisation with DAPI, unaltered in PUV specimens, also implies a high susceptibility to intracellular tissue inhibitor of metalloproteinase (TIMP). TIMP expression was not measured here but is upregulated in adult BOO models [30].

Comparison of PUV with exstrophy bladders. Reduced contractile function, increased passive stiffness and reduced detrusor muscle content are also a feature of detrusor samples from patients with bladder exstrophy [8]. With exstrophy, intracellular Ca^{2+} signalling in detrusor myocytes, in response to contractile agonists such as carbachol is normal. This suggests that

replacement of smooth muscle, and not myocyte failure, underlies contractile failure and that an anti-fibrosis approach to restore function is preferable. The antifibrotic hormone, relaxin, achieves this end in adult bladders rendered fibrotic with X-ray irradiation [31], but there have been to our knowledge no equivalent studies in paediatric bladders. Multiplex immunofluorescence labelling targeted stages in the TFG-β fibrosis pathway and showed, in comparison to normal bladder, reduced β-catenin and c-Myc, as also observed in bladder exstrophy [8]. However, MMP-7 and cyclin-D1 expression was raised in contrast to reduced MMP-7 and unchanged cyclin-D1 in bladder exstrophy. Whether these variations represent fundamentally different pathways in fibrotic development with these different anomalies, and/or different stages in the temporal evolution of their overall phenotype remains to ascertained. However, they do highlight the role of particular cellular pathways in the development of a common pathology.

Limitations

1: The normal group contained a heterogeneous group of patients and it is presumed that there were no significant differences between any subgroups. It may be noted that significant associations between patient age and either contractile function of smooth muscle proportion was seen in this group. 2: It was not possible to carry out each experimental protocol on a particular biopsy sample due to size limitations of the sample. 3: The PUV biopsy samples investigated in this study are from a subset who do not have a decompensated bladder by virtue of the fact the great majority required augmentation cystoplasty or a vesicostomy. Thus, the pathological changes recorded here may not reflect those in those patients have who do show such decompensation.

Conclusions.

The data demonstrate reduced contractile function in bladder wall samples from PUV bladders: a major reason is failure to develop the adult proportional mix of detrusor muscle and extracellular matrix. Increased passive stiffness is consistent with mantained collagen deposition and could underly the low-compliance, poorly contractile phenotype observed in many of these patients and one that is difficult to reproduce in animal models of fetal bladder outflow obstruction. Immunohistochemical data indicate no enhanced role for the Wnt-signalling pathway in this maintenance of fibrosis, but does suggest enhanced cellular remodelling.

Conflicts of Interest

The authors have no conflicts of interest with respect this submission

Acknowledgements

We are grateful for funding from the following sources: The Urological Foundation; The Braithwaite Foundation; The Childrens' Research Fund, Liverpool; The Royal College of Surgeons of England

References

[1] Brownlee E, Wragg R, Robb A, Chandran H, Knight M, McCarthy L. Current epidemiology and antenatal presentation of posterior urethral valves: Outcome of BAPS CASS National Audit. J Ped Surg 2019; 54: 318-321.

[2] Hennus PM, van der Heijden GJ, Bosch JL, de Jong TP, de Kort LM. A systematic review on renal and bladder dysfunction after endoscopic treatment of infravesical obstruction in boys. PLoS One 2012; 7: e44663.

[3] Peters CA, Bolkier M, Bauer SB, Hendren H, Colodny AH, Mandell J, Retik AB (1990): The urodynamicconsequences of posterior urethral valves. J Urol 144:122–126.

[4] Peters CA, Vasavada S, Dator D, Carr M, Shapiro E, Lepor H, McConnell J, Retik AB, Mandell J. The effect of obstruction on the developing bladder. J Urol. 1992; 148: 491-496.

[5] Rohrmann R, Zderic, SA, Duckett JW, Levin RM, Damaser MS. Compliance of the obstructed fetal rabbit bladder. Neurourol Urodyn 1997; 16: 179-189.

[6] Nyirady P, Thiruchelvam N, Fry CH, Godley ML, Winyard PJ, Peebles DM, Woolf AS, Cuckow PM. Effects of in utero bladder outflow obstruction on fetal sheep detrusor contractility, compliance and innervation. J Urol. 2002; 168: 1615-1620.

[7] Farrugia MK, Godley ML, Woolf AS, Peebles DM, Cuckow PM, Fry CH. Experimental short-term partial fetal bladder outflow obstruction: II. Compliance and contractility associated with urinary flow impairment. J Pediatr Urol 2006; 2: 254-260.

[8] Johal NS, Arthurs C, Cuckow P, Cao K, Wood DN, Ahmed A, Fry CH. Functional, histological and molecular characteristics of human exstrophy detrusor. J Pediatr Urol 2019; 15: 154.e1-154.e9

[9] Lan HY, Chung AC. TGF-β/Smad signaling in kidney disease. Semin Nephrol; 32: 236-243.

[10] Chilosi M, Poletti V, Zamò A, Lestani M, Montagna L, Piccoli P, Pedron S, Bertaso M, Scarpa A, Murer B, Cancellieri A, Maestro R, Semenzato G, Doglioni C. Aberrant Wnt/β-catenin pathway activation in idiopathic pulmonary fibrosis. Am J Pathol 2003; 162: 1495-1502.

[11] Shen Y, Miao N, Wang B, Xu J, Gan X, Xu D, Zhou L, Xue H, Zhang W, Yang L, Lu L. c-Myc promotes renal fibrosis by inducing integrin αv-mediated transforming growth factor-β signaling. Kidney Int 2017; 92: 888-899.

[12] Cuevas CA, Tapia-Rojas C, Cespedes C, Inestrosa NC, Vio CP. β-catenin-dependent signaling pathway contributes to renal fibrosis in hypertensive rats. Biomed Int 2015; Article ID 726012

[13] Wang Q, Symes AJ, Kane CA, Freeman A, Nariculam J, Munson P, Thrasivoulou C, Masters JR, Ahmed A. A novel role for Wnt/Ca^{2+} signaling in actin cytoskeleton remodeling and cell motility in prostate cancer. PlosOne 2010; 5: e10456.

[14] Arthurs C, Murtaza BN, Thomson C, Dickens K, Henrique R, Patel HR, Beltran M, Millar M, Thrasivoulou C, Ahmed A. Targets of Wnt/ß-catenin transcription in penile carcinoma. PloS One 2017; 12: e0186047.

[15] Johal N, Wood DN, Wagg AS, Cuckow P, Fry CH. Functional properties and connective tissue content of pediatric human detrusor muscle. Am J Physiol Renal Physiol 2014; 307: F1072-1079.

[16] Wu C, Bayliss M, Newgreen D, Mundy AR, Fry CH. A comparison of the mode of action of ATP and carbachol on isolated human detrusor smooth muscle. J Urol 1999; 162: 1840-1847.

[17] Rohrmann D, Monson FC, Damaser MS, Levin RM, Duckett JW Jr, Zderic SA. Partial bladder outlet obstruction in the fetal rabbit. J Urol 1997; 158: 1071-1074.

[18] Scott RS, Uvelius B, Arner A. Changes in intracellular calcium concentration and $P2X_1$ receptor expression in hypertrophic rat urinary bladder smooth muscle. Neurourol Urodyn 2004; 23: 361-366.

[19] O'Reilly BA, Kosaka AH, Chang TK, Ford AP, Popert R, McMahon SB. A quantitative analysis of purinoceptor expression in the bladders of patients with symptomatic outlet obstruction. BJU Int 2001; 87: 617-622.

[20] Emir H, Eroğlu E, Tekant G, Büyükünal C, Danişmend N, Söylet Y. Urodynamic findings of posterior urethral valve patients. Eur J Pediatr Surg 2002; 12: 38-41.

[21] Puri A, Grover VP, Agarwala S, Mitra DK, Bhatnagar V. Initial surgical treatment as a determinant of bladder dysfunction in posterior urethral valves. Pediatr Surg Int 2002; 18: 438-443.

[22] Thiruchelvam N, Nyirady P, Peebles DM, Fry CH, Cuckow PM, Woolf AS. Urinary outflow obstruction increases apoptosis and deregulates Bcl-2 and Bax expression in the fetal ovine bladder. Am J Pathol 2003; 162: 1271-1282.

[23] Kim JC, Yoon JY, Seo SI, Hwang TK, Park YH. Effects of partial bladder outlet obstruction and its relief on types I and III collagen and detrusor contractility in the rat. Neurourol Urodyn. 2000;19(1):29-42.

[24] Wenger MP, Bozec L, Horton MA Mesquida M. Mechanical properties of collagen fibrils. Biophys J 2007; 93: 1255–1263.

[25] Johnston L, Cunningham RM, Young JS, Fry CH, McMurray G, Eccles R, McCloskey KD. Altered distribution of interstitial cells and innervation in the rat urinary bladder following spinal cord injury. J Cell Mol Med 2012; 16: 1533-1543.

[26] Nevzorova YA, Hu W, Cubero FJ, Haas U, Freimuth J, Tacke F, Trautwein C, Liedtke C. Overexpression of c-myc in hepatocytes promotes activation of hepatic stellate cells and facilitates the onset of liver fibrosis. Biochim Biophys Acta 2013; 1832: 1765-1775.

[27] Chen L, Hou J, Fu X, Chen X, Wu J, Han X. tPA promotes the proliferation of lung fibroblasts and activates the Wnt/β-catenin signaling pathway in idiopathic pulmonary fibrosis. Cell Cycle 2019; 18: 3137-3146.

[28] Klein EA, Assoian RK. Transcriptional regulation of the cyclin D1 gene at a glance. J Cell Sci 2008; 121: 3853-3857.

[29] Deveaud CM, Macarak EJ, Kucich U, Ewalt DH, Abrams WR, Howard PS. Molecular analysis of collagens in bladder fibrosis. J Urol 1998; 160: 1518-1527.

[30] Yang L, Liu R, Wang X, He D. Imbalance between matrix metalloproteinase-1 (MMP-1) and tissue inhibitor of metalloproteinase-1 (TIMP-1) contributes to bladder compliance changes in rabbits with partial bladder outlet obstruction (PBOO). BJU Int 2013; 112: E391-397.

[31] Ikeda Y, Zabbarova IV, Birder LA, Wipf P, Getchell SE, Tyagi P, Fry CH, Drake MJ, Kanai AJ. Relaxin-2 therapy reverses radiation-induced fibrosis and restores bladder function in mice. Neurourol Urodyn 2018; 37: 2441-2451.

Figure legends

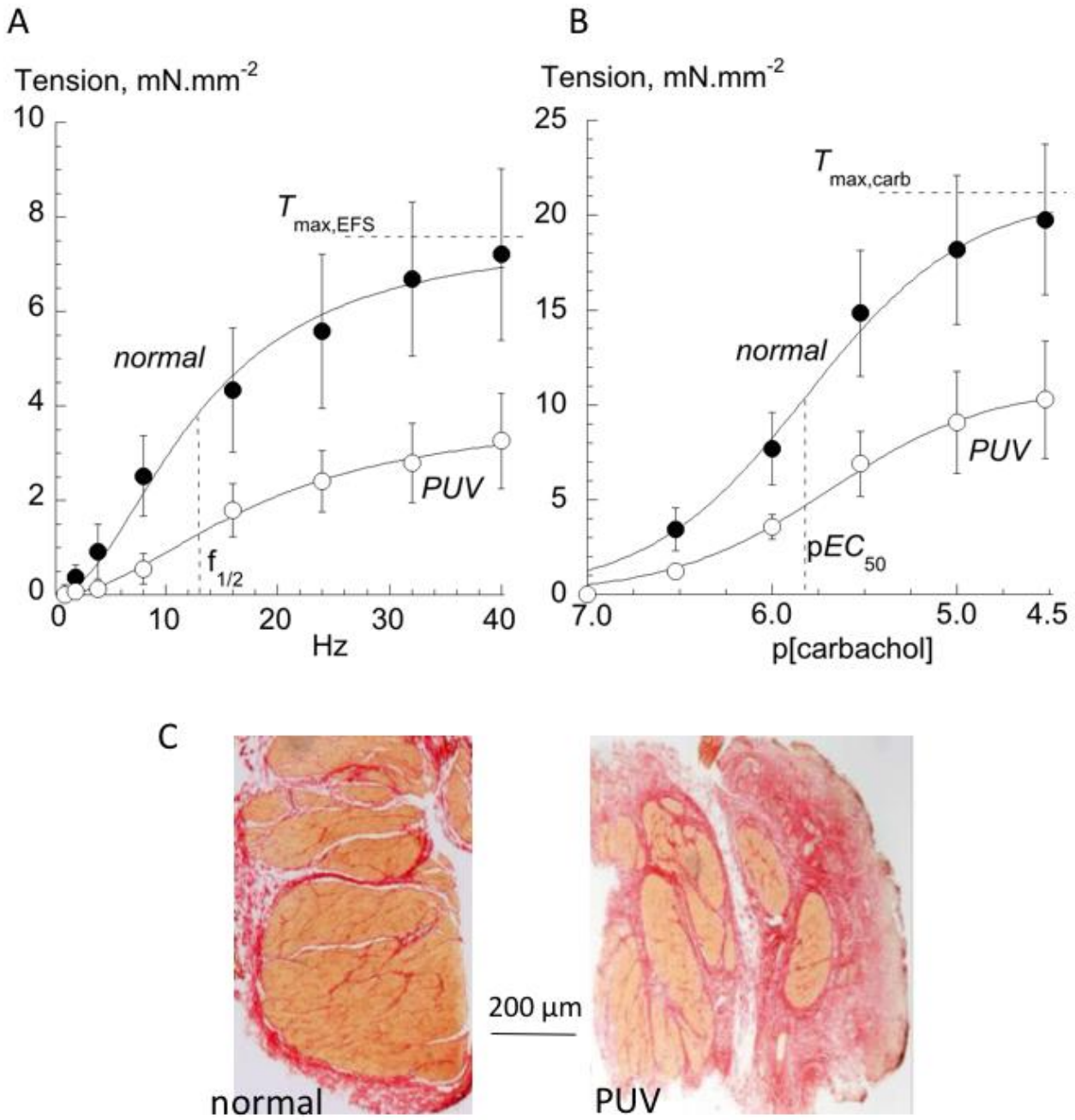

Figure 1. Contractile responses and histology of normal and PUV bladder tissue. A: Frequency-response curves for electrical field stimulation. The horizontal and vertical dotted lines show the best-fit values of $T_{max,EFS}$ and $f_{1/2}$, respectively; N=8,8 (normal, PUV) samples; **B:** Concentration-response curves to carbachol. The horizontal and vertical dotted lines show the best-fit values of $T_{max,carb}$ and EC_{50}, respectively N=8,7 (normal, PUV). Data are mean±SEM. C: Elastin van Gieson stain of normal (left) and PUV (right) bladder sections (orange, smooth muscle; red, collagen).

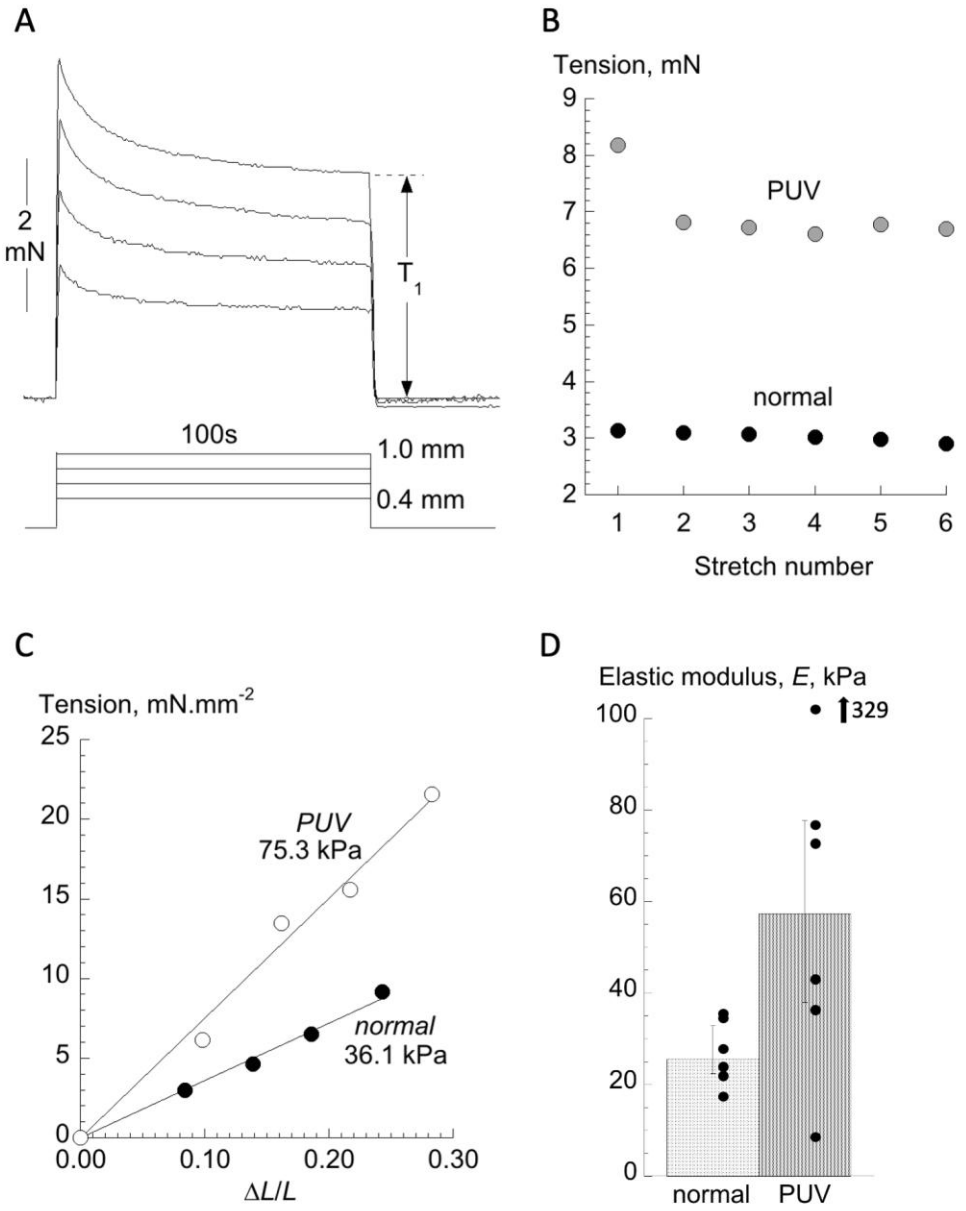

Figure 2. Passive biomechanical properties of bladder wall biopsies. **A:** Superimposed tension (stress) traces in response to rapid strain changes for 100 s, before return to the resting tension. In this example from a normal bladder preparation the proportional strain changes ($\Delta L/L$, L = resting length) were 0.08, 0.12, 0.16 and 0.20. The value of T_1 is shows for the 1.0 mm strain change. **B:** Examples of successive strain changes on steady-state tension, T_1, in preparations from two samples, one each from a normal and PUV bladder sample; the second and third responses were averaged in each preparation. **C:** Two examples of stress (T)-strain ($\Delta L/L$) relationships; the slopes of the lines were used as an estimate of elastic modulus. **D:** Values of elastic modulus in samples from normal and PUV bladders. Mean±SEM data (n=6,5); *p<0.05.

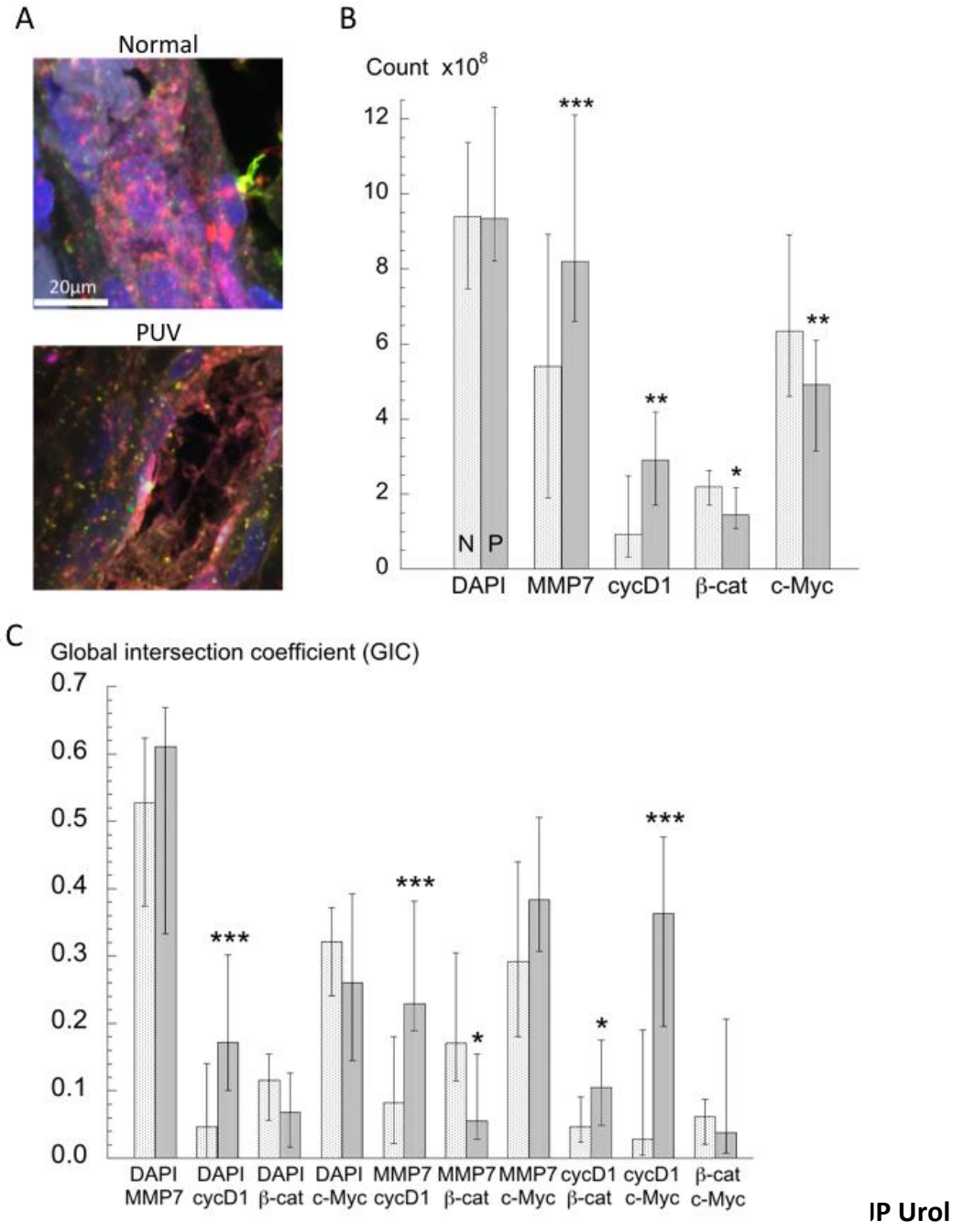

Figure 3. Image analysis of normal and PUV bladder samples. **A:** Multiplex immunofluorescent images of a normal (top) and PUV (bottom) sections (75x75 µm) imaged at x63 with a x6 digital zoom. Images are presented as a maximum intensity Z-stack projection. The following secondary fluorescent labels were used; Cy3 (514/565 nm, yellow, MMP-7), Cy5 (633/671 nm, purple, cyclin-D1), FITC (488/517 nm, green, β-catenin), Cy3.5 (561/617 nm, red, c-Myc) respectively, as well as the nuclear counter-stain DAPI (405/429 nm, blue). **B:** Intensity analysis of normal (*n*=30, *N*=10) and PUV (*n*=21, *N*=7) sections. **C:** Global intersection coefficients between pairs of labels. Mean data±SEM (*n*=10,7). *p<0.05; **p<0.01; ***p<0.001.

Table 1. Age (months), gender and procedures undergone by patients donating tissue. Median age and 25%,75% interquartiles at bottom of column. The type of experiments undertaken are: biomechanics (B); contraction measurements (C); histology (H); Immunofluorescence (I). Procedures - ureteric reimplantation for vesico-ureteric obstruction, reflux or ureterocoele; bladder augmentation and Mitrofanoff; cystoprostatectomy for a rhabdomyosarcoma; bladder diverticulum excision; vesicostomy generation, revision (rev) or closure (cl)

	Normal bladder function					PUV			
Sample	Age	Gender	Procedure	Expts	Sample	Age	Gender	Procedure	Expts
N1	30	M	reimplantation	C	P1	1	M	vesicostomy	H,C
N2	48	F	reimplantation	H,C,I	P2	71	M	augmentation	H,C,I
N3	56	M	reimplantation	H,C,I	P3	183	M	Mitrofanoff	H,C,I
N4	3	M	urachus closure	H,I	P4	24	M	augmentation	H,C,I
N5	56	M	reimplantation	H,C,I	P5	24	M	augmentation	H,C,I
N6	71	F	reimplantation	H,C,I	P6	56	M	augmentation	H,C,I
N7	21	F	reimplantation	H,C,I	P7	105	M	augmentation	H,C,I
N8	19	M	reimplantation	H,C,I	P8	22	M	augmentation	H,I
N9	13	M	reimplantation	H,C,I	P9	70	M	vesicostomy cl	B
N10	33	M	cystoprostatectomy	H	P10	165	M	renal trans	B
N11	18	M	reimplantation	H,C,I	P11	100	M	augmentation	B
N12	54	M	bladder divertic.	H,C,I	P12	187	M	augmentation	B
N13	3	F	vesicostomy	B	P13	94	M	augmentation	B
N14	88	M	vesicostomy rev	B	P14	25	M	vesicostomy	B
N15	156	F	augmentation	B					
N16	39	M	reimplantation	B					
N17	141	M	reimplantation	B					
N18	14	M	reimplantation	B					
median	39	13 M			median	71	14 M		
IQ	[19,56]	5 F			IQ	[24,104]			

Table 2. Contractile characteristics of detrusor muscle from normal and posterior urethral valve (PUV) bladders. Mean data±SEM, except Elastic Modulus data as medians [25,75%] interquartiles; numbers in parenthesis are *n* preparations from *N* biopsy samples. Atropine resistance, % pre-atropine value; pEC_{50} = -logEC_{50}; SM/CT = smooth muscle/connective tissue ratio. *p<0.05; **p<0.01; ***p<0.001.

	Normal	PUV
$T_{max,EFS}$, mN.mm^{-2}	8.0 ± 2.4 (12,9)	3.7 ± 1.2 (9,7) **
$f_{1/2}$, Hz	13.2 ± 2.2 (12,9)	17.9 ± 1.8 (8,7)
Atropine resistance, %	27.1 ± 3.7 (11,8)	21.6 ± 8.4 (6,6)
$T_{max,carb}$ mN.mm^{-2}	19.4 ± 4.3 (11,8)	11.2 ± 4.3 (8,7) *
Carbachol pEC_{50}	5.81 ± 0.12 (11,8)	5.72 ± 0.09 (7,7)
T_{ABMA}, mN.mm^{-2}	11.1 ± 2.5 (11,8)	3.3 ± 1.5 (8,7) **
$T_{max,n-m}/T_{max,carb}$	0.46 ± 0.09 (10,7)	0.51 ± 0.08 (7,7)
SM/CT ratio	3.15 ± 0.64 (11,11)	1.02 ± 0.22 (8,8) ***
Elastic modulus, kPa	25.6 [22.4,32.9] (6,6)	57.3 [38.0,77.7] (6,6) *